Sequence Dependence of 4′,6-Diamidino-2-phenylindole (DAPI)–DNA Interactions

Karl Jansen, Bengt Nordén, and Mikael Kubista*

Contribution from the Department of Physical Chemistry, Chalmers University of Technology, S-412 96 Göteborg, Sweden

*Received June 14, 1993**

Abstract: We have characterized the interaction of 4′,6-diamidino-2-phenylindole (DAPI) with a series of DNA oligonucleotides containing a varying number of contiguous alternating AT base pairs in the center of a GC-stretch. The binding affinity of DAPI to the oligonucleotides increases with the number of contiguous AT base pairs. When entropy effects are taken into account, the microscopic affinity reaches a maximum value when the oligonucleotides contain three AT base pairs. Three is also the minimum number of base pairs that provides a binding site with all the characteristics of binding observed with DNA and $[poly(dA\text{-}dT)]_2$ at low binding ratios. With none or only a single AT base pair in the center of a GC dodecamer, the spectral properties of bound DAPI are very similar to those of DAPI bound to $[poly(dG\text{-}dC)]_2$. When DAPI is complexed with an oligonucleotide containing two AT base pairs, the absorption and fluorescence properties of DAPI closely resemble those of DAPI complexed with $[poly(dG\text{-}dC)]_2$, while the circular dichroism spectrum resembles that of DAPI bound to $[poly(dA\text{-}dT)]_2$.

Introduction

Aromatic diamidino compounds were studied early for their trypanocidal activity,[1] and in an effort to produce better trypanocides, several diamidino compounds were synthesized.[2] Among these, 4′,6-diamidino-2-phenylindole (DAPI) has become the most widely used, though not as a trypanocide but as a DNA probe, owing to its large increase in fluorescence quantum yield upon binding to double-stranded DNA.[3–6] DAPI has been exploited, for example, in cytofluorometry[5,7–13] and for staining chromosomes.[14–16]

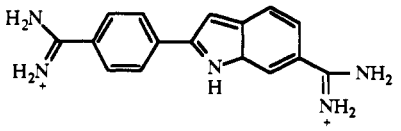

4′,6-diamidino-2-phenylindole (DAPI)

DAPI binds preferably to AT-regions in the minor groove of DNA,[3,14,17–19] and this high-affinity binding mode has been characterized in detail by crystallography.[20] The binding to GC-regions is markedly different from AT binding, and both intercalative[21] and major-groove[22] binding have been proposed. DAPI is not chiral and does not display circular dichroism (CD) when free in solution. However, upon binding to DNA, it acquires strong induced CD owing to interactions with the chiral substrate.[23,24] For ligands bound to DNA, the induced CD is very sensitive to the binding geometry,[24–26] and several different modes of binding can be distinguished for DAPI.[17,23,27] For example, already at low binding ratios, the CD spectrum of DAPI bound to $[poly(dA\text{-}dT)]_2$ starts to change in shape. Among the explanations that have been considered for this phenomenon are allosteric change of the DNA structure induced by the DAPI ligand[19,28] and exciton interactions between close-lying DAPI molecules.[27,29]

In this paper, the binding properties and affinities of DAPI to a series of oligonucleotides with a varying number of consecutive AT base pairs in the center of a GC oligomer are determined. By comparison with the features of DAPI bound to $[poly(dA\text{-}dT)]_2$ and to $[poly(dG\text{-}dC)]_2$, we determined the sequence requirements for the AT minor-groove and GC binding modes of the ligand.

Materials and Methods

Chemicals. All chemicals used were of analytic grade, and aqueous solutions were prepared with deionized triply-filtered water (Millipore).

* Abstract published in *Advance ACS Abstracts*, October 15, 1993.

(1) Ashley, J. N.; Barber, H. J.; Ewins, A. J.; Newbery, G.; Self, A. D. H. *J. Chem. Soc.* **1942**, 103–116.
(2) Dann, O.; Bergen, G.; Demant, E.; Volz, G. *Liebigs Ann. Chem.* **1971**, *749*, 68–89.
(3) Williamson, D. H.; Fenell, D. J. *Methods Cell Biol.* **1975**, *12*, 335–351.
(4) Kapuschinski, J.; Skozylas, B. *Nucleic Acids Res.* **1978**, *5*, 3775–3799.
(5) Williamson, D. H.; Fenell, D. J. *Methods Enzymol.* **1979**, *56*, 728–733.
(6) Cavatorta, P.; Masotti, L.; Szabo, A. G. *Biophys. Chem.* **1985**, *22*, 11–16.
(7) Russel, W. C.; Newman, C.; Williamson, D. H. *Nature* **1975**, *235*, 461–462.
(8) Hajduk, S. L. *Science* **1976**, *191*, 858–859.
(9) Tijssen, J. P. F.; Beekes, H. W.; van Stevenick, J. *Biochem. Biophys. Acta* **1982**, *23*, 679–683.
(10) Lee, G. M.; Thornwaite, J. T.; Rach, E. M. *Anal. Biochem.* **1984**, *137*, 221–225.
(11) Brown, R. N.; Hitchcock, P. F. *Dev. Brain Res.* **1989**, *50*, 123–128.
(12) Chi, H.; Ishibashi, Y.; Shima, A.; Mihara, I.; Osuka, F. *J. Invest. Dermatol.* **1990**, *95*, 154–157.
(13) Takata, K.; Hirano, H. *Acta Histochem. Cytochem.* **1990**, *23*, 679–683.
(14) Lin, M. S.; Comings, D. E.; Alfi, O. S. *Chromosoma* **1977**, *60*, 15–25.
(15) Bernheim, A.; Miglierina, K. *Hum. Genet.* **1989**, *83*, 189–193.
(16) Bella, J. L.; Gosálvez, J. *J. Biotechnol. Histochem.* **1991**, 44–52.
(17) Kubista, M.; Akerman, B.; Nordén, B. *Biochemistry* **1987**, *26*, 4545–4553.
(18) Härd, T.; Fan, P.; Kearns, D. R. *Photochem. Photobiol.* **1990**, *51*, 77–86.
(19) Wilson, W. D.; Tanious, F. A.; Barton, H. J.; Jones, R. L.; Fox, K.; Wydra, R. L.; Strekowski, L. *Biochemistry* **1990**, *29*, 8452–8461.
(20) Larsen, T. A.; Godsell, D. S.; Cascio, D.; Grzeskowiak, K.; Dickerson, R. E. *J. Biomol. Struct. Dyn.* **1989**, *7*, 477–491.
(21) Wilson, W. D.; Tanious, F. A.; Barton, H. J.; Strekowski, L.; Boykin, D. W. *J. Am. Chem. Soc.* **1989**, *111*, 5008–5010.
(22) Kim, S. K.; Eriksson, S.; Kubista, M.; Nordén, B. *J. Am. Chem. Soc.* **1993**, *115*, 3441–3447.
(23) Manzini, G.; Barcellona, M. L.; Avitabile, M.; Quadrifoglio, F. *Nucleic Acids Res.* **1983**, *11*, 8861–8876.
(24) Kubista, M.; Akerman, B.; Nordén, B. *J. Phys. Chem.* **1988**, *92*, 2352–2356.
(25) Lyng, R.; Rodgers, A.; Nordén, B. *Biopolymers* **1991**, *26*, 1709–1720.
(26) Lyng, R.; Rodgers, A.; Nordén, B. *Biopolymers* **1992**, *32*, 1207–1214.
(27) Nordén, B.; Eriksson, S.; Kim, S. K.; Kubista, M.; Lyng, R.; Akerman, B. *The Jerusalem Symposia on Quantum Chemistry and Biochemistry*; Pullman, B., Jortner, J., Eds.; Kluwer Academic Publishers: Dordrecht, 1990; pp 23–41.
(28) Eriksson, S.; Kim, S. K.; Kubista, M.; Nordén, B. *Biochemistry* **1993**, *32*, 2987–2998.
(29) Jansen, K.; Lincoln, P.; Nordén, B. *Biochemistry* **1993**, *32*, 6605–6612.

0002-7863/93/1515-10527$04.00/0

Table I. Oligonucleotide Sequences[a]

no.	sequence	no.	sequence
0	GCGCGCGCGCGC	3	GCGCGTATGCGC
	CGCGCGCGCGCG		CGCGCATACGCG
1	GCGCGCACGCGC	4	GCGCATATGCGC
	CGCGCGTGCGCG		CGCGTATACGCG
2	GCGCGATCGCGC	7	GCGATATATAGCG
	CGCGCTAGCGCG		CGCTATATATCGC

[a] Oligonucleotides **0**–**4** are dodecamers having none to four central AT base pairs; **7** is a tridecamer with seven central AT base pairs.

DAPI was purchased from Serva and used without further purification. The oligonucleotides (Table I) were synthesized on an Applied Biosystems 318A DNA synthesizer, purified with polyacrylamide gel electrophoresis, and, following ethanol precipitation, dissolved in the measurement buffer (100 mM NaCl, 50 mM Tris, pH = 7.4). All concentrations were determined spectroscopically, assuming a molar absorptivity for free DAPI of $\epsilon_{342} = 23\,000\ M^{-1}\ cm^{-1}$.[4] For the single-stranded oligonucleotides, the molar absorptivities were calculated from $\epsilon_{258}/10^3 = 11.7n_G + 7.3n_C + 15.4n_A + 8.8n_T\ M^{-1}\ cm^{-1}$ where n_X is the number of bases of type X in the oligonucleotide.[30] All experiments were performed at 5 °C to minimize strand separation.

Spectroscopic Measurements. Circular dichroism (CD) is defined as

$$\Delta\epsilon(\lambda) = \epsilon_l(\lambda) - \epsilon_r(\lambda) \quad (1)$$

where $\epsilon_l(\lambda)$ and $\epsilon_r(\lambda)$ are the molar absorptivities of left and right circularly polarized light. The circular dichroism spectra were recorded on a Jasco J-720 dichrometer using a 1-cm quartz cell.

Fluorescence-emission spectra were recorded on an Aminco SPF-500 spectrofluorometer, and all spectra were corrected for the inner-filter effect.[31] The quantum yields for the DAPI–polynucleotide complexes were determined using 9,10-diphenylanthracene in cyclohexane as reference (fluorescence quantum yield 0.9).[32]

Determination of Macroscopic Equilibrium Constants. Macroscopic affinity constants were calculated from the standard equilibrium equation

$$K = \frac{[SL]}{[S][L]} \quad (2)$$

assuming the equilibrium

$$S + L \overset{K}{\rightleftarrows} SL \quad (3)$$

where [SL] is the concentration of the DNA–DAPI complex, [S] is the concentration of free oligonucleotide, [L] is the concentration of free ligand, and K is the macroscopic association constant. Equation 2 does not adequately describe the binding to oligonucleotide **7**, which can accommodate two ligands, but the precision in the experimental data is not sufficient to motivate more sophisticated binding models that would have to include interactions between bound ligands. We therefore use eq 2 also for oligonucleotide **7** with $[SL] + 2[SL_2]$ in the nominator, though we emphasize the data points at low-binding occupancies where the concentration of the SL_2 complex is small.

The concentrations of free and bound DAPI were determined from fluorescence-emission spectra. For complexes with low binding affinities, the concentrations were also determined with absorption titrations. To determine the component concentrations in a two-component mixture, it is, in principle, sufficient to measure intensity or absorbance values at two different wavelengths. However, by recording and analyzing whole spectra, the precision in the determination is considerably higher.[33] In our approach, the concentrations were determined from the recorded spectrum $S(\lambda)$ by decomposing it into a linear combination of the spectral responses of free $F(\lambda)$ and bound $B(\lambda)$ ligand:

$$S(\lambda) = aF(\lambda) + bB(\lambda) \quad (4)$$

By normalizing the $S(\lambda)$, $F(\lambda)$, and $B(\lambda)$ spectra with respect to ligand concentration, the coefficients a and b will be the mole fractions of free x_f and bound x_b ligand, respectively, and their sum should equal unity.

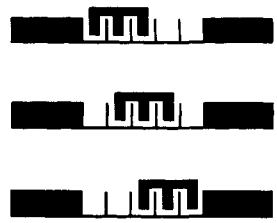

Figure 1. Schematic showing three different ways a ligand, covering three base pairs, can bind to a linear sequence of five base pairs available for binding.

This is the same approach as used by Hagmar *et al.* to determine the binding affinity of methylene blue to DNA and to chromatin.[33] The precision in the determination of the affinity constants is highest when the concentrations of free and bound ligand are about equal. This condition is approached by keeping the total concentrations of both the ligand and the oligonucleotide low in the titration experiments.

As an alternative method to determine binding affinities, we used chemometric analysis, which does not require the spectra of free and bound ligand to be known.[34] This eliminates the uncertainty in the determination of the spectrum of bound ligand, which may be prone to some error owing to nonspecific binding at high ligand concentrations. In this approach, the two most significant principal components for all spectra are calculated using the NIPALS algorithm.[35] The principal components are then "rotated" to produce concentration profiles that satisfy the functional form of the equilibrium expression.[34] In this way, both the affinity constant and the spectral responses of free and bound ligand are determined, and the latter can be compared with the spectra of free and bound ligand used in the first analysis for consistency.

Titrations were initiated with solutions containing DAPI at a concentration of about 10^{-6} M, to which aliquots of a DNA stock solution were added. The range from no binding to essentially quantitative binding was covered in 10–15 additions. After each addition, the samples were mixed thoroughly using a small motor-driven Teflon stirrer. To ensure that the samples were at equilibrium at all stages, it was checked that two spectra recorded at an interval of a few minutes were indentical.

Microscopic and Macroscopic Affinity Constants. When a ligand binds to a DNA oligomer containing more base pairs in continuum, of the kind to which the ligand has high affinity, than the number of base pairs comprising a binding site, there are more potential microscopic sites for the ligand to bind. This increases the binding affinity. If the ligand binds to n base pairs and the sites contain m such base pairs in continuum, the number of microscopic binding sites is $m - n + 1$.[36] As an example, consider a DNA oligomer with five such base pairs in continuum and a ligand that binds to three (Figure 1). The number of microscopic binding sites is then three, and the macroscopic affinity of the ligand to this oligomer will be three times larger than that to an oligomer containing a binding site of three contiguous base pairs. The microscopic affinity constant k is defined as the affinity constant to an oligomer with a single microscopic binding site. The macroscopic affinity constant K to an oligomer having a site of m base pairs is then $K = (m - n + 1)k$.

As the number of base pairs in continuum increases, the number of microscopic binding sites will also increase. For example, with 100 base pairs in continuum, the number of microscopic binding sites for a ligand covering three base pairs is 98, *i.e.*, roughly the number of base pairs. Microscopic affinity constants, not macroscopic, are therefore comparable to the affinity constants determined for long polymers when expressed per base pair.

Results

Absorption. The absorption spectra of DAPI bound to the different oligonucleotides fall into two classes (Figure 2). DAPI bound to oligonucleotides **0**–**2** has spectra characterized by a large hypochromicity (~40% compared to free DAPI) and a large red shift (~20 nm), which are similar to the spectrum of DAPI bound to $[poly(dG\text{-}dC)]_2$.[22] Although the features change somewhat with increasing number of AT base pairs, they are

(30) Sambrook, J.; Fritsch, E. F.; Maniatis, T. *Molecular Cloning, A Laboratory Manual*, 2nd ed.; Cold Spring Harbor Laboratory Press: Cold Spring Harbor, NY, 1989.
(31) Lakowicz, J. R. *Principles of Fluorescence Spectroscopy*; Plenum Press: New York, 1983.
(32) Hamai, S.; Hirayama, F. *J. Phys. Chem.* **1983**, *87*, 83–89.
(33) Hagmar, P.; Pierrou, S.; Nielsen, P. E.; Nordén, B.; Kubista, M. *J. Biomol. Stuct. Dyn.* **1992**, *9*, 667–679.
(34) Kubista, M.; Sjöback, R.; Albinsson, B. *Anal. Chem.* **1993**, *65*, 994–998.
(35) Scarminio, I.; Kubista, M. *Anal. Chem.* **1993**, *65*, 409–416.
(36) McGhee, J. D.; von Hippel, P. H. *J. Mol. Biol.* **1974**, *86*, 469–489.

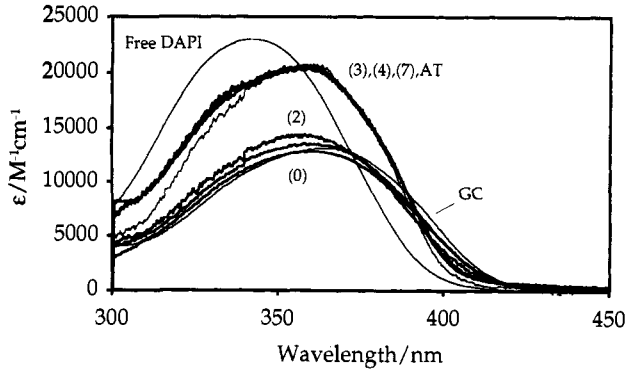

Figure 2. Absorption spectra of DAPI bound to oligonucleotides **0–7**. The absorption profiles of free DAPI and DAPI bound to $[poly(dA-dT)]_2$ and to $[poly(dG-dC)]_2$ are shown for comparison (thin lines).

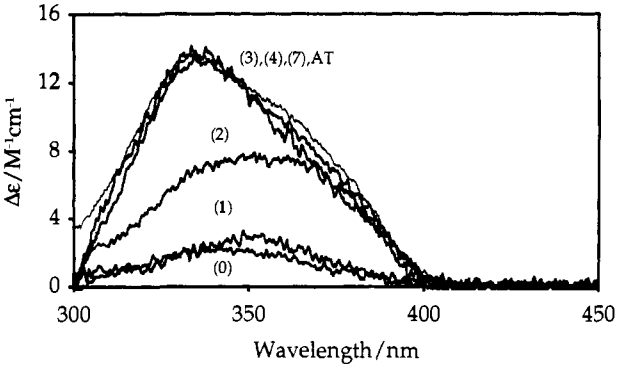

Figure 3. Circular dichroism spectra of DAPI bound to oligonucleotides **0–7**. The profile of DAPI bound to $[poly(dA-dT)]_2$, normalized to the same $\Delta\epsilon$ as **7**, is shown for comparison (thin line).

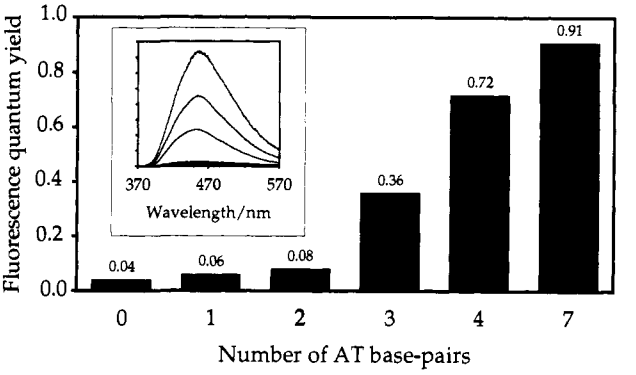

Figure 4. Fluorescence quantum yields for oligonucleotides **0–7**. The insert shows the corresponding emission spectra (using 360-nm excitation).

clearly different from the DAPI spectra obtained with oligonucleotides **3–7**. The latter spectra show much less hypochromicity (~10%) and are similar to the spectrum of DAPI bound to $[poly(dA-dT)]_2$.[28] With oligonucleotide **7**, which can bind two DAPI ligands simultaneously, the same absorption spectrum is observed with one and two ligands bound.

Circular Dichroism. The CD spectra of DAPI bound to the oligonucleotides (Figure 3) fall into three classes. With oligonucleotides **0** and **1**, the CD is rather weak and similar to that of DAPI bound to $[poly(dG-dC)]_2$,[27] whereas with oligonucleotides **3–7**, the CD is strong and the spectral shape is the same as that for DAPI bound to DNA and to $[poly(dA-dT)]_2$ at low ratios.[17,23,27] With oligonucleotide **2**, the CD intensity is in between that of **0** and **1** and **3–7**.

Fluorescence. The fluorescence properties of bound DAPI, presented in Figure 4, are analyzed from two somewhat different angles. In the bar diagram, the fluorescence quantum yields of DAPI bound to the oligonucleotides are shown. The quantum

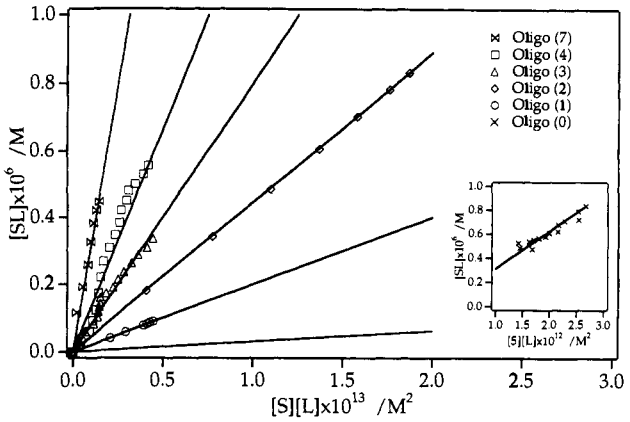

Figure 5. Plot of the concentration of bound DAPI [SL] versus the product of free oligonucleotide concentration and free DAPI concentration [S][L]. The slopes are the macroscopic affinity constants K. The insert shows binding to oligonucleotide **0**, measured with absorption using higher total concentrations (note the different scales).

yield is a measure of the probability that an absorbed photon is emitted as fluorescence and reflects properties of the excited state of DAPI in the complex. The insert shows the fluorescence-emission spectra of bound DAPI and reflects the amount of light emitted per bound ligand. Since the ligands have different molar absorptivities in the various complexes at the given excitation wavelength, the fluorescence quantum yields are not proportional to the integrated emission spectra.

Also here the oligonucleotides fall into two groups. Complexes with **0–2** have a low fluorescence quantum yield, of the same order as that of free DAPI in solution, whereas complexes with **3–7** are highly fluorescent.

Binding Affinities. The equilibrium eq 2 can be written as

$$[SL] = K[L][S] \qquad (5)$$

From this follows that a plot of the product of the concentrations of free DAPI [L] and free DNA [S] versus the concentration of bound ligand [SL] should give a straight line with slope K. The experimental points, shown in Figure 5, can for all oligomers be well fitted with a straight line.

For oligonucleotide **0**, which does not contain any AT base pairs, the DAPI affinity is considerably weaker than those for the other oligonucleotides. Already with oligonucleotide **1**, which contains a single AT base pair, the binding constant is substantially larger. Clearly, a single AT base pair has a large effect on the DAPI affinity. For oligonucleotides **2–7**, the macroscopic affinity constant increases with increasing length of the AT segment.

Discussion

Our results on the binding of DAPI to synthetic oligomers reveal several important aspects of the interactions of this drug with DNA, which possibly apply also to other minor-groove binding ligands.

Binding Modes. Our spectroscopic results show that three contiguous AT base pairs are required to obtain all the properties of the so-called binding mode I, observed for DAPI bound to DNA and $[poly(dA-dT)]_2$ at low binding ratios.[17,27] Even though DAPI bound to oligonucleotide **2** has a CD similar to that of mode I binding and the ligand is probably located in the minor groove as judged by NMR,[37] the binding differs from that of longer AT sequences, as evidenced by our absorption, fluorescence, and binding affinity data. This is consistent with footprinting studies,[38,39] which showed that a binding site of three to four AT base pairs is required for high binding affinity.

(37) Trotta, E.; D'Ambrosio, E.; Del Grosso, N.; Ravagnan, G.; Cirilli, M.; Paci, M. *J. Biol. Chem.* **1993**, *268*, 3944–3951.
(38) Portugal, J.; Waring, M. J. *Biochim. Biophys. Acta* **1988**, *949*, 158–168.
(39) Jeppesen, C.; Nielsen, P. E. *Eur. J. Biochem.* **1989**, *182*, 437–447.

Table II. Fluorescence Quantum Yields and Binding Affinities of DAPI for the Different Oligonucleotides and Polynucleotides

substrate	fluorescence quantum yield	macroscopic affinity constant	microscopic affinity constant[a]	binding mode[a]
0	0.04	3.1×10^5	*e*	GC
1	0.06	1.2×10^6	1.2×10^6	GC
2	0.08	4.5×10^6	2.7×10^6	intermediate
3	0.36	8.0×10^6	8.0×10^6	AT
4	0.72	1.3×10^7	6.9×10^6	AT
7	0.91	3.2×10^7	6.6×10^6	AT
DNA	0.90[c]		1.4×10^5 (1.3×10^7)[f,g]	AT
[poly(dA-dT)]$_2$	0.90		5.6×10^5 (5×10^7)[f,h]	AT
[poly(dG-dC)]$_2$	0.04		1.2×10^5[i]	GC
free DAPI	0.043[d]			

[a] Binding affinity per potential site; see text for details. Binding affinities to long polymers are expressed as M^{-1} bp^{-1}. [b] As inferred from CD spectra. [c] References 4 and 43. [d] Reference 18. [e] The entropic effect is difficult to account for; see text. [f] Affinity constant to B-DNA and within parentheses, to allosterically altered DNA; see text. [g] Reference 42. [h] Estimated from Wilson et al.[19] [i] Reference 19.

The increase in the fluorescence intensity of DAPI upon binding to DNA has been proposed to be due to shielding of the dye from water molecules.[40] DAPI bound to oligonucleotides **0**–**2** should thus be accessible to water, whereas when it is bound to oligonucleotides **3** to **7**, the accessibility should be considerably hindered. The gradual increase in fluorescence quantum yield when going from oligonucleotide **3**–**7** indicates that there is still some accessibility to water in **3** and **4**. In **7**, the fluorescence quantum yield is as high as that in [poly(dA-dT)]$_2$ (Table II). A plausible explanation for the lower yield in **3** and **4** could be that the "binding pocket" in these oligomers is not large enough to close up tightly around the ligand.

We conclude that DAPI binds to oligonucleotide **1**, containing a single AT base pair, in a similar manner as to [poly(dG-dC)]$_2$. To oligonucleotides **3**–**7**, containing at least three contiguous AT base pairs, DAPI binds in the same way as to [poly(dA-dT)]$_2$ and DNA at low binding ratios in mode I. The binding of DAPI to oligonucleotide **2**, having two AT base pairs, falls in between these two extremes.

The observation that the absorption and CD spectra of DAPI are the same with one and two ligands bound to oligonucleotide **7** suggests that the binding modes in the oligonucleotide **7**–DAPI and oligonucleotide **7**–DAPI$_2$ complexes are equivalent.

Binding Affinities. The macroscopic binding affinity to the oligonucleotides increases with increasing length of the AT segment. For oligonucleotides **3**–**7**, the increase can be explained as an entropy effect, owing to a larger number of microscopic binding sites in longer AT-stretches.[36] The microscopic affinity constant of DAPI to these oligomers, assuming a microscopic binding site of three AT base pairs, is about the same, 7×10^6 M^{-1} (Table II).

It is not straight forward to compare the microscopic affinity constant of DAPI for the AT-rich oligonucleotides with those determined for DNA and [poly(dA-dT)]$_2$ because of the allosteric change of the DNA molecule induced when several DAPI ligands bind in close proximity which leads to an increase in affinity.[28] In the oligonucleotides studied here, no allosteric change is observed, as expected, since a single bound ligand is not sufficient to alter the DNA structure.[28] The microscopic affinity constants we determined are those of DAPI binding to a site in normal DNA and correspond to the affinity constant K_1 in the allosteric binding model of Dattagupta *et al.*[41] Wilson *et al.* analyzed the binding of DAPI to [poly(dA-dT)]$_2$ in terms of the allosteric model and estimated K_1 and K_2 to be 5.6×10^5 and 5×10^7 M^{-1}, respectively, at our experimental conditions.[19] Their value of K_1 is thus about 10 times lower than what we determined for monomeric binding. The reason for this discrepancy is most likely that their value is too low, owing to the uncertainty in fitting a single binding isotherm using the many parameters required by the allosteric model. Another possible source of error might be that the model they used does not take into account interactions between bound ligands. Since DAPI is doubly charged (2+), ligands bound in close proximity will repel each other electrostatically. Although these effects may be incorporated in the allosteric model,[28] they introduce additional parameters, making a fit to experimental data unstable.

The binding affinities we obtained are about an order of magnitude lower than those reported by Loontiens *et al.*[42] for similar oligonucleotides. We presently have no satisfactory explanation for this discrepancy. When we tried their approach, based on single-point analysis of fluorescence data, we were unable to obtain reproducible results. In fact, this was the reason why we redesigned our experiments to record and analyze complete spectra. The affinity constants determined by Loontiens *et al.*[42] are not only higher than ours but are significantly higher than any affinity constants for DAPI reported earlier, which also the authors noted. Their values are even higher than the K_2 constant reported by Wilson *et al.*, which requires a conformational change of the DNA lattice and is about 90 times larger than the affinity constant to normal B-form DNA.[19]

For oligonucleotide **0**, which contains only GC base pairs, there is, of course, also an entropic effect as a result of many potential microscopic binding sites. Here, the effect is more difficult to account for, since all GC base pairs are unlikely to be equivalent owing to end effects. If they were equivalent, the entropic effect should give a macroscopic affinity constant that is 8–12 times larger, depending on the site size, than the affinity constant observed with [poly(dG-dC)]$_2$. The binding affinity for DAPI to [poly(dG-dC)]$_2$ is about 1.2×10^5 M^{-1} under our conditions,[19] which is only three times lower than the macroscopic affinity constant we observed for oligonucleotide **0**. This suggests that DAPI binds preferentially to the central base pairs in the oligonucleotide, which is reasonable owing to the expected lower electrostatic potential in the middle of the oligonucleotide.

Both oligonucleotides **1** and **2** bind one DAPI ligand. In oligonucleotide **1**, there is a single AT base pair and consequently only one microscopic site. In oligonucleotide **2**, there are two microscopic sites of length one AT base pair and, relative to oligonucleotide **1**, the entropic effect is expected to give twice as large an affinity. Taking this into account, we find that the affinity for oligonucleotide **2** is still about two times higher than that for oligonucleotide **1**, suggesting that the interaction with two consecutive AT base pairs is more advantageous than that with two isolated AT base pairs.

In conclusion, we find that a single AT base pair increases the affinity of DAPI for DNA considerably. The affinity increases further with a second and third contiguous AT base pair. Most of the properties of the high-affinity binding mode observed with [poly(dA-dT)]$_2$ and DNA are observed with a binding site of three AT base pairs. The only exception is the fluorescence intensity which increases in larger AT-stretches and reaches a maximum value first with more than four contiguous AT base pairs.

Acknowledgment. This project was supported by the Swedish Natural Science Research Council (NFR) and the Swedish Council for Engineering Sciences (TFR).

(40) Barcellona, M. L.; Gratton, E. *Eur. Biophys. J.* **1990**, *17*, 315–323.
(41) Dattagupta, N.; Hogan, M.; Crothers, D. M. *Biochemistry* **1980**, *19*, 5998–6005.
(42) Loontiens, F. G.; McLughlin, L. W.; Diekmann, S.; Clegg, R. M. *Biochemistry* **1991**, *30*, 182–189.
(43) Barcellona, M. L.; Favilla, R.; von Berger, J.; Avitabile, M.; Ragusa, N.; Masotti, L. *Arch. Biochem. Biophys.* **1986**, *250*, 48–53.